Polarized laser spectroscopy and crystal-field analysis of Er^{3+} doped $CaGdAlO_4$

Polarized laser spectroscopy and crystal-field analysis of Er^{3+} doped $CaGdAlO_4$

Jon-Paul R Wells†‖, Mitsuo Yamaga‡ Nobuhiro Kodama§ and
Thomas P J Han†

† Optical Materials Research Centre, Department of Physics and Applied Physics,
University of Strathclyde, Glasgow G1 1XN, Scotland, UK
‡ Department of Electronics, Faculty of Engineering, Gifu University, Gifu 501-1193, Japan
§ Department of Materials Science and Engineering, Faculty of Engineering and
Resource Science, Akita University, 1-1 Tegatagakuen, Akita 010-8502, Japan

E-mail: wells@huygens.rijnh.nl

Abstract. A single Er^{3+} centre in $CaGdAlO_4$:Er^{3+} has been identified to have C_{4v} symmetry from polarized laser selective excitation. This is consistent with isovalent substitution of the Er^{3+} ions for host crystal Gd^{3+} ions. Using both optical and infrared absorption and polarized laser excited fluorescence, 59 crystal-field energy levels and their wavefunction symmetries have been identified and used to perform comprehensive single electron crystal-field analyses for the Er^{3+} ion centre. For excitation of the $^4F_{9/2}$ multiplet, blue and green upconversion fluorescence is observed. Self-absorption dips recorded in upconversion excitation spectra are indicative of the presence of radiative energy transfer processes.

1. Introduction

$CaGdAlO_4$ (CGA) is a crystal which crystallizes in the perovskite phase, with tetragonal K_2NiF_4 structure. As such, the D_{4h}^{17} space group is appropriate for this material. CGA belongs to a wide family of isomorphs having the general formula $ABCO_4$ [1–7] where A denotes an alkaline earth cation, B denotes Y, Sc or a trivalent rare earth element and C corresponds to Al, Ga or a transition metal ion. In this structure, the C exist in slightly distorted octahedral sites stacked in layers perpendicular to the c-direction. Between the layers, the divalent A and trivalent B cations reside in ninefold co-ordinated sites which have distorted C_{4v} symmetry due to the random occupation of neighbouring sites by Ca^{2+} and Gd^{3+}.

The overwhelming majority of spectroscopic studies of the $ABCO_4$ family of materials has been directed towards the $SrLaAlO_4$ and $CaYAlO_4$ host crystals. In both the optical and electron paramagnetic resonance spectra [4, 8] of Ce^{3+} doped into $CaYAlO_4$, the inherent substitutional disorder was found to give rise a distribution of non-C_{4v} electrostatic crystal-field potentials at the Ce^{3+} ion site. This was found to lead to a distribution of Ce^{3+} $^2F_{5/2}$ ground state magnetic splitting factors and to a broadening of the parity-allowed $5d^1 \rightarrow 4f^1$ spectral line profiles as measured in fluorescence. A similar inhomogeneous broadening has been observed

‖ Corresponding author. Current address: Dr Jon-Paul R Wells, FELIX Free Electron Laser Facility, FOM—Institute for Plasmaphysics 'Rijnhuizen', Edisonbaan 14, 3430 BE Nieuwegein, The Netherlands.

for optical spectroscopy of the intra-4f transitions of Pr^{3+}, Nd^{3+} and Eu^{3+} doped $SrLaAlO_4$ crystals [3, 9, 10]. In these studies, it was also shown that despite the lowered symmetry of the surroundings of the rare-earth ion (the substitutional disorder causes the C_4 axis of the C_{4v} centre to be tilted away from the crystalline *c*-axis) there is no accompanying reduction of the well defined polarization behaviour of the RE^{3+} ion transitions. The assertion was made that the ensemble of RE^{3+} ions behaves as a single 'quasi-centre' because single exponential radiative decay times were observed.

As a consequence of the disordered nature of this family of crystals $ABCO_4$, there is some interest in these compounds as laser gain media because the broadened inhomogeneous linewidths allow the tuning range of laser oscillation to widen (however the gain is also distributed over a larger bandwidth). Demonstrations of laser operation have been performed in both $CaYAlO_4$:1% Nd^{3+} [11] and $CaYAlO_4$:2% Tm^{3+} [12] with 20–50 mW output at 1.080 μm and 1.970 μm respectively. More recently, 360 mW output power has been achieved at a wavelength of 1.078 μm from a $CaGdAlO_4$:2% Nd^{3+} laser crystal using a 1.29 W GaAlAs diode pump source at 806.5 nm [13]. Quite apart from applications as laser gain media, these compounds have been employed as substrate materials for superconducting thin films [14]. Indeed, the construction of high temperature superconducting bolometers has been reported with a sensitive element constructed from a superconducting $YBa_2Cu_3O_7$ film on a $CaGdAlO_4$ substrate [15].

In this paper we report on crystal-growth, optical absorption, laser excitation and fluorescence studies of $CaGdAlO_4$:Er^{3+}. We have also attempted to detect electron paramagnetic resonance signals from the Er^{3+} ions in this crystal; however no resonances could be obtained due to the strong signals from Gd^{3+} which is stoichiometrically incorporated into the lattice. Gd^{3+} ions influence the energy levels of Er^{3+} through exchange interaction, resulting in line-broadening of optical spectra. From a combination of optical absorption and laser excited fluorescence we have determined 59 experimental energy levels of the single Er^{3+} ion centre in this material. A good account of these experimental data is provided in terms of a single electron crystal-field analysis. The spectroscopic properties of this material are compared and contrasted to those of $SrLaAlO_4$:Er^{3+} [16] and $CaYAlO_4$:Er^{3+} [1].

2. Crystal growth

$CaGdAlO_4$ crystals doped with 1 and 5 mol% Er^{3+} were grown in an inert atmosphere of argon gas by the Czochralski technique from charges of stoichiometric composition, which assume substitution of the Er^{3+} ion dopant for Gd^{3+}. The oxide powders of $CaCO_3$ (4N purity) and Gd_2O_3, Er_2O_3 and Al_2O_3 (5N purity) were weighed out and then mechanically mixed for three hours. The mixed powders were placed in a rubber bag and then pressed at 1500 kg cm^{-2} under a hydrostatic press. The pressed samples were melted by inductive heating at 1953–2093 K in an iridium crucible of dimensions 46 mm in diameter by 48 mm in height. These were homogenized for several hours before the seed was immersed. The $CaGdAlO_4$:Er^{3+} crystals were grown along the [100] axis at pulling rates of 0.8–2 mm h^{-1} and a crystal rotation rate of 10 rpm. The compositions of the as grown crystals were determined by inductively coupled plasma (ICP) emission analysis which yielded the exact compositions as $Ca_{0.98}Gd_{0.01}Er_{1.01}Al_{0.99}O_4$ and $Ca_{0.96}Gd_{0.97}Er_{0.04}Al_{1.02}O_4$. The as-grown crystals were optically transparent and showed a uniform pink colouring due to the Er^{3+} ion dopant. The resulting boules were cut and polished into samples with approximate dimensions for optical measurements, the cut faces being normal to [100], [010] and [001] directions.

3. Experiment

Absorption spectra were recorded with an AVIV associates 14DS double beam spectrophotometer with crystals cooled to a base temperature of 10 K using a Leybold cryogenic refrigeration unit. Laser excitation and fluorescence spectra were recorded using a 5 W Coherent Innova 70 argon ion laser to optically pump a Spectra-Physics 375B dye laser with rhodamine 560 dye dissolved in 100% ethyl-glycol. The sample was cooled by a CTI-cryogenics model 22C cryogenic refrigerator and temperature variability was maintained by a Palm Beach Cryogenics temperature controller. For fluorescence wavelengths in the range 400–800 nm, a Hamamatsu R9249 photomultiplier, which was thermoelectrically cooled to $-25\,^{\circ}$C, was used to detect the light. For near infrared light, a liquid nitrogen cooled germanium detector was used with phase sensitive detection provided by an Ortholoc model 9502 lock-in amplifier. Polarization spectra were recorded with a polaroid sheet with a Hanle wedge employed to correct for the differing response of the spectrometer to different polarizations. Schott glass filters were used to avoid second order diffraction complicating spectra recorded in the 1000–1500 nm region. Fluorescence lifetimes were recorded using a Laser Science Inc VSL-337 nitrogen laser pumped dye laser with Coumarin 503 and DCM. The transient was recorded with a Stanford Research Systems model SR430 multichannel averager. The integrated transients were least squares fitted to single exponential decays on a constant background for the fluorescence decay times.

4. Spectroscopy of CaGdAlO$_4$:Er^{3+}

The 4f^{11} configuration, appropriate for trivalent erbium, has a total of 364 electronic states in 41 free-ion multiplets. As a consequence of Kramers theorem, there exists a twofold residual degeneracy that cannot be removed by a time reversal invariant field such as the electrostatic environment provided by the SrLaAlO$_4$ host crystal [16]. As such, there exist 182 twofold degenerate electronic energy levels prior to the application of an external magnetic field.

Erbium ion multiplets are labelled either by the leading $^{2S+1}L_J$ term in the intermediate coupled free-ion wavefunction or by the single letter notation which follows Dieke [17]. The individual crystal-field levels of a given multiplet are labelled by both the appropriate letter for that multiplet and by a numerical subscript, in sequence from the lowest energy level of the multiplet. Thus, the Er^{3+} ^{4}I$_{15/2}$ multiplet is labelled Z with the ground state labelled Z$_1$, the first excited state Z$_2$ and so on.

4.1. Optical absorption

The absorption spectra of 14 Er^{3+} ion multiplets between 6000 and 30 000 cm^{-1} have been recorded with a 6.2 mm thick CaGdAlO$_4$:1% Er^{3+} sample, cooled to 10 K. These are shown in figure 1 with individual transitions labelled according to their appropriate numerical subscript. These show a marked resemblance to those presented for SrLaAlO$_4$:Er^{3+} [16] and CaYAlO$_4$:Er^{3+} [1] as might be expected for isomorphic host materials. In these materials, the compositional disorder inherent in the crystalline structure gives rise to a strong inhomogeneous broadening of the spectral lines of rare-earth ion dopants. In spite of this, the crystal-field levels of nearly all of the spectra shown in figure 1 are fully resolved with 47 individual transitions observed. The measured linewidths of these transitions are comparable to those reported for SrLaAlO$_4$:1% Er^{3+} at close to 40 cm^{-1} (a value averaged over all of the observed transitions). The measured linewidths are not concentration dependent up to the highest concentration
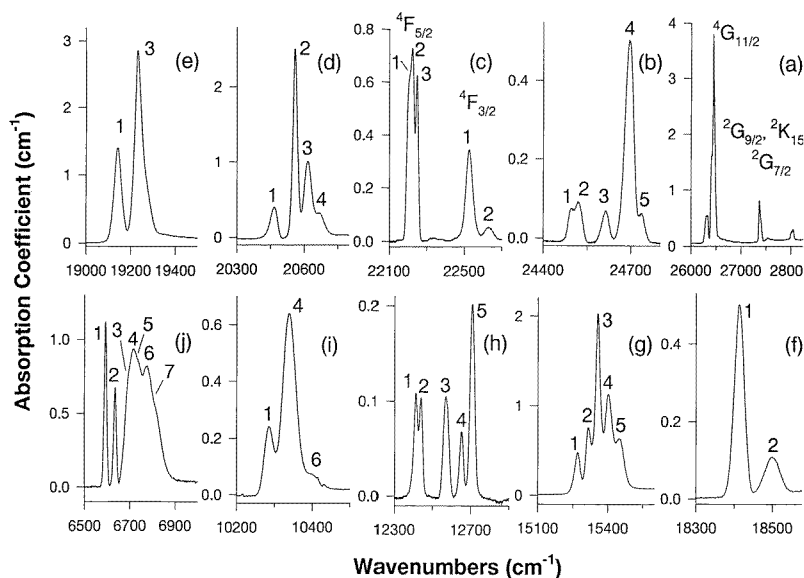
Figure 1. 10 K absorption spectra for the (a) $^4G_{11/2}$, $^2G_{9/2}$, $^2K_{15/2}$ and $^2G_{7/2}$, (b) $^2H_{9/2}$, (c) $^4F_{5/2}$ and $^4F_{3/2}$, (d) $^4F_{7/2}$, (e) $^2H_{11/2}$, (f) $^4S_{3/2}$, (g) $^4F_{9/2}$, (h) $^4I_{9/2}$, (i) $^4I_{11/2}$ and (j) $^4I_{13/2}$ multiplets of CaGdAlO$_4$:1% Er^{3+}. Transitions are labelled by the appropriate numerical subscript of the terminating state.

studied of 5 mol% and it is concluded that the magnitude of this observable is dominated by contributions from the compositional disorder in the crystal. However, it is possible that a contribution to the broadening can be made by exchange interactions between the electron spins of Er^{3+} and the Gd^{3+} ligands (see for example [18]).

4.2. Laser excited fluorescence

A medium resolution ($\sim$1 cm^{-1} linewidth) rhodamine 560 dye laser has been used to excite the $^4S_{3/2}$ multiplet of Er^{3+} in CaGdAlO$_4$. Unlike SrLaAlO$_4$:Er^{3+}, only the single ion C$_{4v}$ symmetry centre could be identified in CaGdAlO$_4$:Er^{3+}. Figure 2 shows polarized laser excited fluorescence spectra for this spectroscopic centre, obtained exciting the $(^4I_{15/2})Z_{1\gamma7} \rightarrow (^4S_{3/2})E_{2\gamma6}$ transition at 18 499 cm^{-1}. Fluorescence transitions from the $^4S_{3/2}$, $^4F_{9/2}$, $^4I_{11/2}$ and $^4I_{13/2}$ multiplets are observed. Despite the broadened spectral linewidths, in most cases all transitions to the $J + \frac{1}{2}$ crystal-field levels of the lower multiplets are observed. Figure 2(f) shows the $^4I_{13/2} \rightarrow {}^4I_{15/2}$ transitions. This spectrum is cut at close to 6400 cm^{-1} as this is at the long wavelength limit of the Spex 500 monochromator's drive. A shoulder is observed on the $(^4I_{13/2})Y_{1\gamma7} \rightarrow (^4I_{15/2})Z_{1\gamma7}$ transition. This is unidentified but is not related to the fluorescence of a different Er^{3+} ion centre.

Figures 3(a)–(c) show fluorescence spectra recorded for frequencies above that of the exciting DCM dye laser (under 15 356 cm^{-1} excitation of the $^4F_{9/2}$ multiplet). These transitions emanate from the $^2P_{3/2}$, $^2H_{9/2}$ and $^4S_{3/2}$ multiplets and result from Er^{3+} ion upconversion processes. Figure 4 shows the excitation spectra of the $^4F_{9/2}$ multiplet monitoring upconversion at 18 412 cm^{-1} (figure 4(a)), 21 111 cm^{-1} (figure 4(b)) and monitoring fluorescence below the laser line at 14 810 cm^{-1} (figure 4(c)). For all three spectra, those transitions below 15 550 cm^{-1} match the $^4I_{15/2} \rightarrow {}^4F_{9/2}$ ground state absorption (GSA) transitions. It is
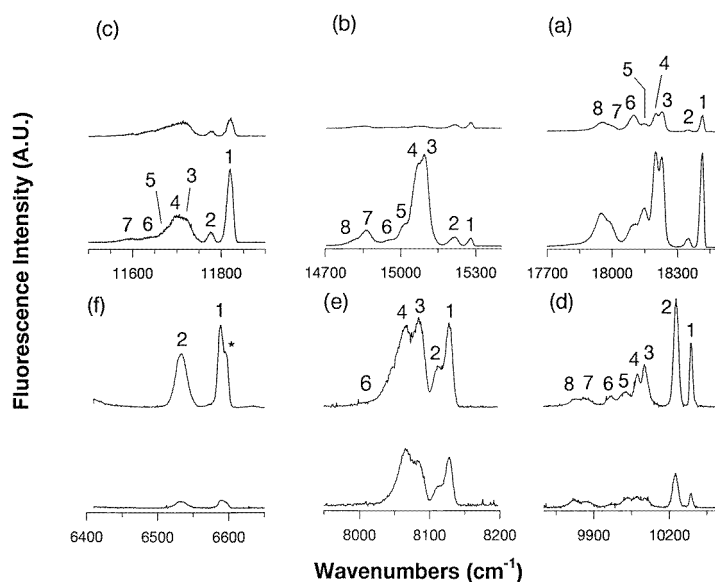
Figure 2. 10 K polarized fluorescence spectra for the (a) $^4S_{3/2} \to {}^4I_{15/2}$, (b) $^4F_{9/2} \to {}^4I_{15/2}$, (c) $^4S_{3/2} \to {}^4I_{13/2}$, (d) $^4I_{11/2} \to {}^4I_{15/2}$, (e) $^4S_{3/2} \to {}^4I_{11/2}$ and (f) $^4I_{13/2} \to {}^4I_{15/2}$ transitions in CaGdAlO₄:1% Er³⁺. The upper spectrum is the σ polarized spectrum whilst the lower is π polarized. The * notation indicates an unassigned feature.
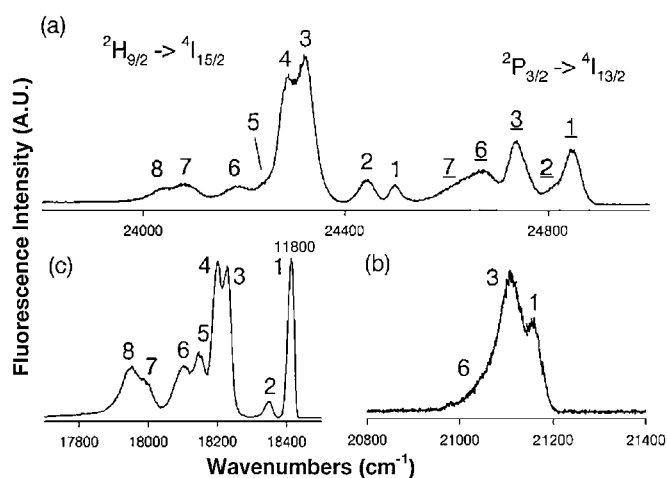
Figure 3. 10 K upconverted fluorescence spectra for the (a) $^2P_{3/2} \to {}^4I_{13/2}$ and $^2H_{9/2} \to {}^4I_{15/2}$, (b) $^2P_{3/2} \to {}^4I_{11/2}$ and (c) $^4S_{3/2} \to {}^4I_{15/2}$ transitions. In (a) the underline notation is used to denote transitions from $^2P_{3/2}$ while those emanating from $^2H_{9/2}$ are not underlined.

particularly noticeable in figure 4(c) that the some of the spectral-line profiles have unusual shapes. This is a consequence of self-absorption (and hence radiative energy transfer) within the crystal at these high concentrations of Er³⁺. For figures 4(a) and (b), additional transitions are observed at higher frequencies than 15 550 cm⁻¹. These transitions correspond to excited state absorption (ESA) transitions from $^4I_{13/2} \to {}^4F_{5/2}$ and $^4F_{3/2}$.

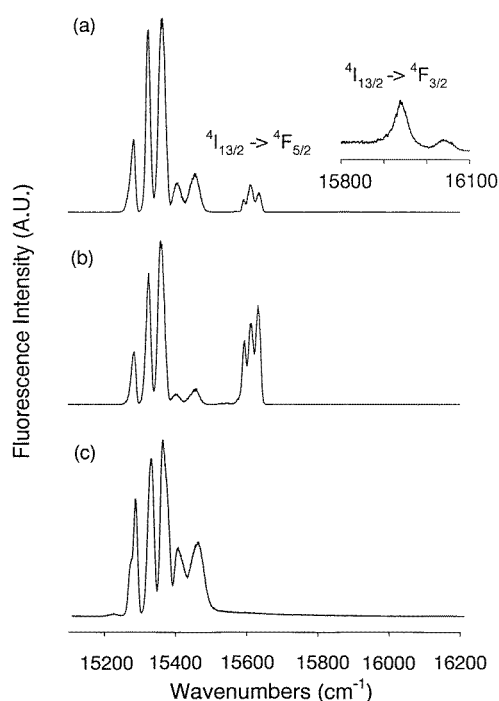**Figure 4.** 10 K excitation spectra for the $^4F_{9/2}$ multiplet monitoring at (a) 18 412 cm^{-1}, (b) 21 111 cm^{-1} and (c) 14 810 cm^{-1}.

The upconversion fluorescence which is emitted from $^4S_{3/2}$ involves the absorption of two photons. The observation of ESA transitions at exactly the energy mismatch between $^4I_{13/2}$ and $^4F_{5/2}$ or $^4F_{3/2}$ clearly indicates that $^4I_{13/2}$ behaves as an intermediate state for this process. This is not an unreasonable assertion as it would be expected that $^4I_{13/2}$ is metastable (e.g. in CaYAlO$_4$:Er^{3+} $\tau(^4I_{13/2}) \approx 6$ ms [1]) and thus the probability of the absorption of a second photon from this state would be high. Clearly, when the laser is resonant with the ESA transitions, the energy mismatch between the GSA and ESA transitions must be made up by the emission of lattice phonons.

The highest frequency fluorescence emanates from the $^2P_{3/2}$ multiplet, whose lowest (and emitting) state is at 31 433 cm^{-1}. Due to the energy of the exciting laser this upconversion process is, by necessity, a three photon process. As similar ESA transitions are observed for the upconversion excitation spectra recorded monitoring the 21 111 cm^{-1} ($^2P_{3/2} \rightarrow {}^4I_{11/2}$) fluorescence, it is clear that the pumping cycle for this fluorescence is identical to that for the green fluorescence with the addition of an additional step. As the $^4F_{5/2}$ state is not long lived, we reasonably assume that the second intermediate state for this process is the $^4S_{3/2}$ multiplet. Thus the second absorbing state is the $^4G_{7/2}$ multiplet at around 33 500 cm^{-1}, which is assisted by phonon sideband absorption to make up the energy mismatch between the laser frequency and that of the excited state absorption transition. Both processes are shown schematically in figure 5(a).

Figures 5(b) and (c) give the dependence of the two upconversion processes upon excitation intensity. Ideally, it would be expected that the power dependence of the green upconversion would be 2, and that of the blue upconversion would be 3. As can be seen in figures 5(b) and

(a)

(b)

(c)
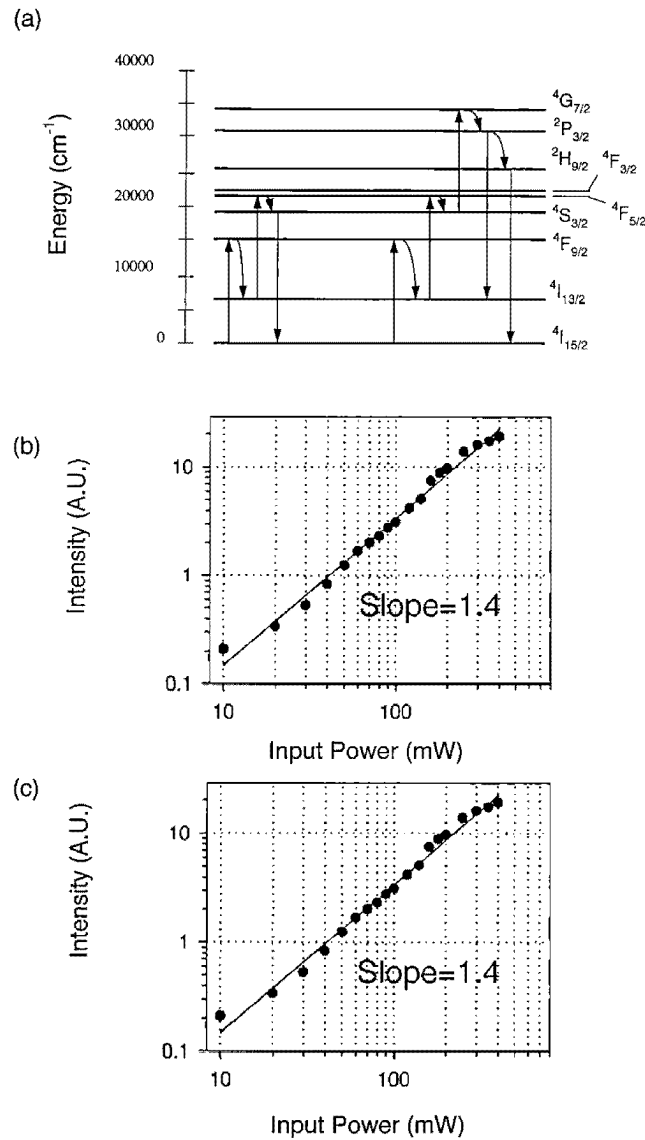
Figure 5. (a) A schematic (and simplified) energy level diagram for the Er^{3+} energy levels under $35\,000$ cm^{-1} indicating the upconversion processes observed here. (b) The dependence of the $18\,412$ cm^{-1} upconversion fluorescence upon power and (c) the dependence of the $21\,111$ cm^{-1} upconversion fluorescence upon power.

(c), both dependences are degraded from the optimum with values of 1.4 and 1.9 measured for the green and blue upconversion respectively. Such behaviour is not unusual at high dopant concentrations where energy transfer processes begin to play an important role in the optical pumping cycle of rare-earth doped compounds (see for example [19], [20]). Evidence of radiative energy transfer processes [21] is provided in the recorded excitation spectra shown in figure 4 where absorption 'dips' are observed. These correspond to the reabsorption of $^4F_{9/2}$ fluorescence by non-excited Er^{3+} ions.

The 10 K fluorescence decay rates of the $^4S_{3/2}$ and $^4F_{9/2}$ multiplets were measured for the C_{4v} symmetry centre with CaGdAlO$_4$ crystals doped with 1 and 5 mol% of trivalent erbium. At both concentrations single exponential decays were observed. The 10 K lifetime of the $^4S_{3/2}$ multiplet was measured to be 168 ± 10 μs for the 1% sample and 148 ± 10 μs for the 5% sample, whilst for the $^4F_{3/2}$ multiplet, a fluorescence lifetime of 9.7 ± 5 μs was measured for the 1% sample, and 7.6 ± 5 μs for the 5% sample. The decay lifetimes measured for the CaGdAlO$_4$:1% Er^{3+} sample compare well with those values measured previously for the C_{4v} centre in SrLaAlO$_4$:1% Er^{3+} of $\tau(^4S_{3/2}) = 234 \pm 10$ μs and $\tau(^4F_{9/2}) = 18 \pm 5$ μs. The longer lifetime measured in SrLaAlO$_4$:Er^{3+} results from the larger ionic radii of the host cations (e.g. Sr^{2+} 1.12 Å, Ca^{2+} 0.99 Å) which, in the case of SrLaAlO$_4$, provide a reduction in the axial distortion experienced by the Er^{3+} ion, thereby lowering its electric dipole transition moment.

5. Crystal-field analysis of the C$_{4v}$ symmetry centre in CaGdAlO$_4$:Er^{3+}

To perform the crystal-field analyses presented here, the *f-Shell Empirical* crystal-field fitting routines of Dr Mike Reid of the University of Canterbury, NZ were used. In analysing the energy level structure of the Er^{3+} ion for the C_{4v} symmetry centre observed here, the free ion and crystal-field Hamiltonian matrices for the entire f^{11} configuration were diagonalized simultaneously. In this manner, we include all intermediate coupling and crystal-field J-mixing effects. The free-ion Hamiltonian is parametrized as follows [22]:

$$H_{c.f.} = \sum_{k=2,4,6} F^k f_k + \sum_i \zeta l_i s_i + \alpha L(L+1) + \beta G(G_2) + \gamma G(R_7)$$
$$+ \sum_{h=0,2,4} M^h m_h + \sum_{k=2,4,6} P^k p_k + \sum_{i,2,3,4,6,7,8} T^i t_i. \tag{1}$$

The predominant terms in this Hamiltonian are the electrostatic and spin–orbit interactions represented by parameters F^k and ζ which are varied in the fit. The remaining terms represent smaller interactions which nevertheless play an important role in the accurate description of the energy level structure of rare-earth ions. These are the configuration interactions (α,β,γ), spin–spin and spin–other-orbit interactions, represented by the parameters M^h, the two body electrostatically correlated magnetic interactions, with parameters P^k, and the three particle configuration interactions, T^i. These are not varied at all, but rather are held constant at the values given in [22].

The appropriate Hamiltonian for C$_{4v}$ symmetry is:

$$H_{c.f.} = B_0^2 C_0^{(2)} + B_0^4 C_0^{(4)} + B_0^6 C_0^{(6)} + B_4^4 (C_4^{(4)} + C_{-4}^{(4)}) + B_4^6 (C_4^{(6)} + C_{-4}^{(6)}) \tag{2}$$

where the $C_q^{(k)}$ are the Racah spherical tensors as defined in [23]. The fitted and experimental energy levels of the single ion C$_{4v}$ centre are given in table 1, representing the crystal-field energy levels of all free ion multiplets under 32 000 cm^{-1}. Table 1 also lists the assigned wavefunction symmetries in terms of the irreducible representations of the energy levels. As can be seen, good agreement between experiment and theory is obtained. The optimized parameters for the 59 experimental levels of the C$_{4v}$ centre are given in table 2. In fitting the data for the centre, the crystal-field (B_q^k), spin–orbit (ζ) and Coulombic (F^k) parameters were allowed to freely vary with the remaining free-ion interaction parameters held at those obtained for LaF$_3$:Er^{3+} in [22]. Also listed in table 2, are the optimized crystal-field parameters for the C$_{4v}$ symmetry centres in SrLaAlO$_4$:Er^{3+} [16] and CaYAlO$_4$:Er^{3+} [1]. The close comparison between these results gives confidence in the analysis performed here.

Table 1. Fitted and experimental energy levels (in air cm^{-1}, ± 1), for the C$_{4v}$ symmetry centres in CaGdAlO$_4$:Er^{3+}.

Multiplet	State	Symmetry	Calc	Expt	Multiplet	State	Symmetry	Calc	Expt
	Z_1	γ_7	−5.4	0		G_1	γ_6	20449.5	20472
	Z_2	γ_6	55.1	63		G_2	γ_7	20549.9	20563
	Z_3	γ_6	198.9	183	$^4F_{\frac{7}{2}}$	G_3	γ_7	20608.7	20620
	Z_4	γ_7	224.6	222		G_4	γ_6	20659.2	20672
$^4I_{\frac{15}{2}}$	Z_5	γ_6	287.3	267		H_1	γ_7	22178.3	22205
	Z_6	γ_7	319.3	312	$^4F_{\frac{5}{2}}$	H_2	γ_7	22217.6	22216
	Z_7	γ_6	439.0	434		H_3	γ_6	22233.8	22242
	Z_8	γ_7	462.9	461	$^4F_{\frac{3}{2}}$	I_1	γ_7	22504.1	22524
	Y_1	γ_7	6593.5	6591		I_2	γ_6	22602.8	22623
	Y_2	γ_6	6636.1	6633		K_1	γ_7	24482.8	24485
	Y_3	γ_6	6715.7	6708		K_2	γ_6	24500.7	24505
$^4I_{\frac{13}{2}}$	Y_4	γ_7	6740.5	6710	$^2H_{\frac{9}{2}}$	K_3	γ_6	24594.7	24599
	Y_5	γ_6	6748.2	6733		K_4	γ_7	24693.8	24682
	Y_6	γ_7	6791.2	6767		K_5	γ_6	24718.6	24723
	Y_7	γ_7	6842.2	6815		L_1	γ_7	26336.6	26308
	A_1	γ_7	10262.0	10285		L_2	γ_6	26342.7	26327
	A_2	γ_6	10282.2	10299		L_3	γ_7	25428.4	26411
	A_3	γ_6	10323.3	10329	$^4G_{\frac{11}{2}}$	L_4	γ_6	26543.8	26444
$^4I_{\frac{11}{2}}$	A_4	γ_7	10330.3	10346		L_5	γ_7	26476.3	26464
	A_5	γ_6	10352.0	—		L_6	γ_6	26503.9	—
	A_6	γ_7	10391.7	10397		M_1	γ_6	27385.3	27365
	B_1	γ_7	12372.2	12411		M_2	γ_7	27390.7	27388
	B_2	γ_6	12412.7	12439	$^4G_{\frac{9}{2}}$	M_3	γ_6	27413.2	—
$^4I_{\frac{9}{2}}$	B_3	γ_6	12535.0	12571		M_4	γ_6	27432.8	—
	B_4	γ_7	12625.3	12651		M_5	γ_7	27443.3	—
	B_5	γ_6	12672.4	12709		N_1	γ_7	27546.1	27505
	D_1	γ_6	15279.8	15271		N_2	γ_6	27550.5	—
	D_2	γ_6	15322.2	15316		N_3	γ_7	27654.7	—
$^4F_{\frac{9}{2}}$	D_3	γ_7	15372.6	15356		N_4	γ_6	27659.9	—
	D_4	γ_7	15422.4	15401	$^2K_{\frac{15}{2}}$	N_5	γ_6	27756.7	—
	D_5	γ_6	15461.8	15450		N_6	γ_7	27795.5	—
	E_1	γ_7	18398.7	18412		N_7	γ_7	27872.5	—
$^4S_{\frac{3}{2}}$	E_2	γ_6	18480.9	18499		N_8	γ_6	28113.7	—
	F_1	γ_7	19168.5	19142		O_1	γ_6	27979.1	27992
	F_2	γ_6	19173.9	—		O_2	γ_7	28010.3	—
	F_3	γ_7	19226.8	19232	$^2G_{\frac{7}{2}}$	O_3	γ_7	28026.4	28021
$^2H_{\frac{11}{2}}$	F_4	γ_6	19241.7	—		O_4	γ_6	28037.5	—
	F_5	γ_7	19273.2	—	$^2P_{\frac{3}{2}}$	P_1	γ_7	31443.0	31433
	F_6	γ_6	19290.3	—		P_2	γ_6	31583.1	—

6. Conclusions

We have reported upon the spectroscopy of compositionally disordered CaGdAlO$_4$ crystals doped with trivalent erbium ions. Using low temperature absorption and polarized laser excited fluorescence techniques we have identified the single Er^{3+} ion centre in this material as having C$_{4v}$ symmetry consistent with substitution for host lattice Gd^{3+} ions. Single electron

Table 2. Optimized free-ion and crystal-field parameters for the C_{4v} symmetry centres in $CaGdAlO_4:Er^{3+}$, $SrLaAlO_4:Er^{3+}$ and $CaYAlO_4:Er^{3+}$. All values are in cm^{-1} (except n, the number of experimental points). Those values in square brackets have been not been varied but instead have been held at the values of Carnall *et al* [22].

Parameter	CGA:Er^{3+}	SLA:Er^{3+}	CYA:Er^{3+}
F^2	98 659	98 328	
F^4	69 701	70 851	
F^6	48 972	48 967	
α	[17.79]	[17.79]	
β	[−582.1]	[−582.1]	
γ	[1800]	[1800]	
T^2	[400]	[400]	
T^3	[43]	[43]	
T^4	[73]	[73]	
T^6	[−271]	[−271]	
T^7	[308]	[308]	
T^8	[299]	[299]	
M^{tot}	[3.86]	[3.86]	
P^{tot}	[594]	[594]	
ζ	2364	2365	
B_0^2	698	760	704
B_0^4	367	363	476
B_4^4	−597	−379	−396
B_0^6	−164	−179	−297
B_4^6	792	734	722
σ	19.8	13.9	
n	59	40	

crystal-field analyses of the 59 measured energy levels of the Er^{3+} ion give close account of the experimental data and yield physically reasonable parameters consistent with those of isomorphic host lattices. Strong upconversion fluorescence is observed for excitation of the $^4F_{9/2}$ multiplet with a single DCM dye laser.

Acknowledgments

References

[1] Hutchinson J A, Verdun H R, Chai B H T, Zandi B and Merkle L D 1994 *Opt. Mater.* **3** 287
[2] Yamaga M, Takeeuchi H, Holliday K, Macfarlane P, Henderson B, Inoue Y and Kodama N 1995 *Radiat. Eff. Defects Solids* **135** 223
[3] Ryba-Romanowski W, Brenier A, Garapon C and Gloubokov A 1995 *Appl. Phys.* B **61** 345
[4] Kodama N, Yamaga M and Henderson B 1996 *J. Phys.: Condens. Matter* **8** 3505
[5] Woensdregt C F, Janssen H W M, Gloubokov A and Pajaczkowska A 1997 *J. Cryst. Growth* **171** 392
[6] Jezierski A 1998 *Phys. Status Solidi* b **207** 183
[7] Yamaga M, Yosida T, Naitoh Y and Kodama N 1994 *J. Phys.: Condens. Matter* **6** 4381
[8] Yamaga M, Kodama N, Yosida T, Henderson B and Kindo K 1997 *J. Phys.: Condens. Matter* **9** 9639

[9] Ryba-Romanowski W, Golab S, Dominiak-Dzik G, Pajaczkowska A and Berkowski M 1994 *J. Physique Coll.* IV C **4** 561

[10] Ryba-Romanowski W, Golab S, Pisarki W A, Domainiak-Dzik G, Berkowski M and Pajaczkowska A 1997 *J. Phys. Chem. Solids* **58** 639

[11] Stephens E, Schearer L D and Verdun H R 1992 *Opt. Commun.* **90** 79

[12] Moncorge R, Garnier N, Kerbrat Ph, Wyon Ch and Borel C 1997 *Opt. Commun.* **141** 29

[13] Lagatskii A A, Kuleshov N V, Shcherbitskii V G, Kleptsyn V F, Mikhailov V P, Ostroumov V G and Huber G 1997 *Quantum Electron.* **27** 15

[14] Young K H and Chai B H T 1991 *Japan. J. Appl. Phys.* **30** L2116

[15] Zerov V Y, Leonov V N, Sosnenko M V, Khrebtov I A and Ivanov A A 1998 *J. Opt. Technol.* **65** 242

[16] Wells J P-R, Yamaga M, Mosses R W, Han T P J, Gallagher H G and Yosida T *Phys. Rev.* B submitted

[17] Dieke G H 1968 *Spectra and Energy Levels of Rare Earth Ions in Crystals* (New York: Wiley-Interscience)

[18] Yamaga M, Macfarlane P I, Holliday K, Henderson B, Kodama N and Inoue Y 1997 *J. Phys.: Condens. Matter* **9** 1575

[19] Tallant D R, Miller M P and Wright J C 1976 *J. Chem. Phys.* **65** 510

[20] Brenier A and Jurdyc A M 1995 *J. Lumin.* **65** 45

[21] Noginov M A 1997 *Appl. Opt.* **36** 4153

[22] Carnall W T, Goodman G L, Rajnak K and Rana R S 1989 *J. Chem. Phys.* **90** 3443

[23] Wybourne B G 1965 *Spectroscopic Properties of Rare Earths* (New York: Wiley-Interscience)